

Numerical Studies of Drag reduction on Circular Cylinder With V- Grooves

Munendra C V , Anusha Inamdar, Ranjeeth Kumar

Department of Mechanical Engineering, M. S. Engineering College, Bangalore-562110

munendracv610@gmail.com and 9916389037

Abstract—This work is carried out to investigate the flow structure around a circular cylinder with V- grooves numerically. Drag coefficient and turbulence statistics of wake behind each cylinder were analyzed for Reynolds number based on the cylinder diameter ($D = 40\text{mm}$) in the range $Re_D = 2 \times 10^4$. The V- type grooves reduce the drag coefficient acting on the cylinder by 28.47% at $Re_D = 2 \times 10^4$, compared with that of smooth cylinder at the same Reynolds number. The results were compared with that of a smooth cylinder having the same diameter and the fluid flow characteristics of wake behind the V- grooved cylinder have been analyzed. However, for the case of V- grooved cylinder, the vortices are largely distorted and spread out significantly as they go downstream and the longitudinal grooves seem to shift the location of span wise vortices toward the cylinder, reducing the vortex formation region as compared to the smooth cylinder. The pressure and velocity contours were ensemble averaged to get the spatial distributions of turbulent statistics including turbulent intensities and turbulent kinetic energy. In case of smooth cylinder, large-scale vortices formed behind the cylinder maintain round shape and do not spread out noticeably in the near wake. The sharp peaks of longitudinal V- shaped grooves also suppress the formation of large-scale secondary stream wise vortices and reducing turbulent kinetic energy near-wake region and the secondary vortices are broken into smaller eddies.

Keywords— Circular cylinder, V-Grooves, Drag coefficient, Pressure distribution, Turbulence, velocity vector, stream lines

1. INTRODUCTION

Flow around a circular cylinder was intentionally studied in the past and that returns to its simple geometry as well as the logical structure of the vortices. The studies were led on the one hand by academic interest and on the other hand by practical interest (industrial). In general there are two types to reduce the drag force namely “active control and passive control”. The active control methods order the flow by ensuring external energy by means such as the acoustic excitation or the jet blow. The passive control methods order the flow by modifying the shape of the body or by attaching additives devices such as elements of roughness on the body. The active control requires complex mechanics devices which provide the external power to the flow consequently, the passive method is simpler and easier to realize.

Experimental and numerical investigations have showed a reduction in the drag when using longitudinal grooves namely 2 and 6 on the cylinder [1]. The unsteady incompressible flow fields around smooth and grooved circular cylinders have been simulated by solving the Navier-Stokes equations with appropriate boundary conditions. The groove effects are approximated by a “slip” velocity on the cylinder surface, instead of the conventional “non-slip” boundary condition for smooth cylinders, provided that three dimensionality of the whole flow field and interaction between the grooves and fluids near the surface [2]. Flow structure of wake behind a circular cylinder with longitudinal U- grooves has been investigated experimentally using PIV velocity field measurement techniques. The U- grooved cylinder reduces the drag coefficient by about 18.6%, compared with the smooth cylinder at $Re_D = 1.4 \times 10^5$. The drag reduction of the U- grooved cylinder increases with increasing Reynolds number. The vortex formation region behind U- grooved cylinder is smaller than for the smooth cylinder [3]. The incompressible flow around pairs of circular cylinders in tandem arrangements was investigated. The spectral element method is employed to carry out two- and three-dimensional simulations of the flow. The centre-to-centre distance (l_{cc}) of the investigated configurations varies from 1.5 to 8 diameters (D), and results thus obtained are compared to the isolated cylinder case. Covering the transition in the wake the simulations are in the Reynolds number (Re) range from 160 to 320 and this analysis focuses on the small-scale instabilities of vortex shedding, which occurs in the Re range investigated [4]. It is demonstrated that the total groove area has a significant effect on reducing the critical Reynolds number, whether the area is increased through changing the groove shape, width, or depth. Drag reductions may be realized for circular cylinders in cross-flow by using grooves, even at very shallow relative groove depths. A strong correspondence to the minimum drag coefficient is also observed [5]. Studied on viscous flow past two circular cylinders of different diameters is simulated by using a finite element method. The diameter ratio between the small cylinder and the large one is 0.25. The Reynolds number based on the diameter of the

cylinders is 500 for the large cylinder and 125 for the small cylinder & the gap between the small cylinder and the large cylinder ranges from 0.05 to 1.0 times the diameter of the large cylinder. The position angle of the small cylinder relative to the flow direction ranges from 0 to π . The effects of the gap ratio between the two cylinders and the position angle of the small cylinder on drag and lift coefficients, pressure distributions around the cylinders, the vortex shedding frequencies from the two cylinders and flow characteristics are investigated [6]. The viability and accuracy of large-eddy simulation (LES) with wall modeling for high Reynolds number complex turbulent flows is investigated by considering the flow around a circular cylinder in the supercritical regime. The results are compared with those obtained from steady and unsteady Reynolds-averaged Navier–Stokes (RANS) solutions and the available experimental data. The LES solutions are shown to be considerably more accurate than the RANS results. The boundary layer separation and reduced drag coefficients consistent with experimental measurements after the drag crisis. The mean pressure distribution is predicted reasonably well at $Re_D = 5 \times 10^5$ and 10^6 [7]. Flow past cactus-shaped cylinders are performed at Reynolds numbers of 20, 100, and 300. The results are contrasted to those from smooth cylinders at the same Reynolds numbers. The cavities in the cactus-shaped cylinders are seen to reduce the forces acting on them. At Reynolds number of 20, the drag is reduced by 22% due to reduction in the viscous forces. At Reynolds number of 100, the unsteady pressure forces increase, while the unsteady viscous forces acting on the cactus-shaped cylinder decrease. The overall reduction in drag force is about 18%. At Reynolds number of 300, onset of three dimensionality is observed together with significant decrease in pressure and viscous forces. Both the mean and fluctuating forces are found to decrease considerably. The Strouhal number is also found to decrease by about 10%. These reductions in force magnitudes and observed wake instabilities are attributed to the presence of large-scale, quiescent, recirculating flow within the cactus cavities [9]. The flow around a circular cylinder in air stream, a rod was set upstream of the circular cylinder. The diameter of cylinder, D , was 40 mm, and the diameter of rod, d , ranged from 1 to 10 mm. The distance between the axes of the circular cylinder and rod, L , was 50 – 120 mm. The Reynolds number based on D ranged from 1.5×10^4 to 6.2×10^4 . Two flow patterns with and without vortex shedding from the rod occurred. The flow pattern changes depending on the rod diameter, its position and the Reynolds number. The optimum conditions of the drag reduction are $d/D = 0.25$, $L/D = 1.75 - 2.0$, in these conditions, vortices do not shed from the rod and the shear layer from the rod reattaches on the front face of the circular cylinder. The reduction of the total drag including the drag of the rod is 63% compared with that of a single cylinder [10]. Reductions in drag and fluctuating forces for a circular cylinder by attaching rings. Cylindrical rings were attached along the span of a cylinder at an interval of several diameters to reduce the drag and fluctuating forces caused by fluid flow. Experiments were performed at Reynolds numbers based on the cylinder diameter d ranging between $Re_d = 3000$ for 38 000. The aspect ratio of the cylinder, L/d , was approximately 20. The experimental results revealed that the drag force on the ring-attached cylinder was lower than for the 2D cylinder, even though the projected area was higher. The optimum ring configuration for drag reduction was found to be $D/d = 1.3$, $W/d = 1.0$, and $P/d = 6$ at $Re_d = 30\ 000$, where D is the ring diameter, W is the span wise width of the ring, and P is the spanwise pitch of the ring. This configuration reduced the drag force by 15%. The considerable drag reduction was attributed to the formation of separation bubbles on both sides of the ring in the $Re_d > 410\ 000 - 20\ 000$ range. This in turn, lead to the narrowing of the wake behind the ring and the pressure recovery at the rear of the ring. The fluctuating lift, which was estimated from the fluctuating surface pressures, was also reduced in this range of Reynolds numbers due to the suppression of vortex shedding.

2. NUMERICAL STUDY

The geometry consists of an infinite cylinder mounted horizontally on the side walls where the two ends are fixed (the vibration effects are not considerate here). The downstream length and the upstream length are set at 11.5 of diameter; the origin of the Cartesian coordinate system is located at the centre of the base of the cylinder, the complete geometry is shown in Fig.2.1. The geometry and the boundary conditions remain the same for all tested cylinders.

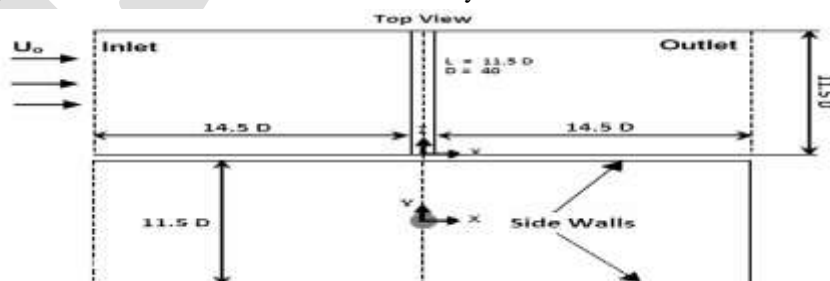


Fig.2.1: Geometry under consideration of infinite cylinder

The geometry carried out numerically corresponds perfectly to the dimensions of the experimental work [1]. In the present study the turbulence models was tested “ $k - \epsilon$ standard”. The grids have been tested for the case of $Re 2 \times 10^4$ and $AR = 11.5$ and that for the smooth cylinders.

2.1 MESHING GEOMETRY OF A SMOOTH CIRCULAR CYLINDER

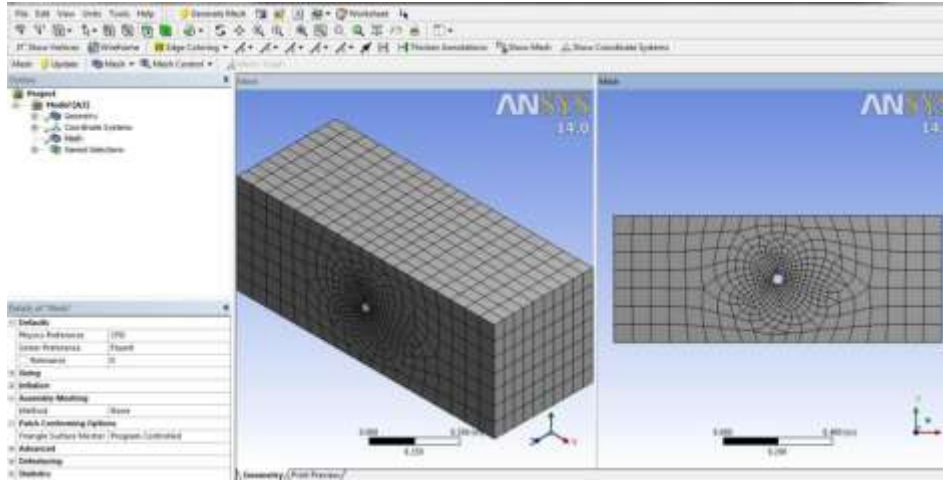


Fig.2.2: Meshing and name selection of meshing for smooth circular cylinder



Fig.2.3: Meshed smooth circular cylinder captured from the rectangular flow domain

ANSYS FLUENT was used for making 3D geometry of smooth surface cylinder with different groove type and angle. For L/D of 11.5 the diameter was taken to be 40mm. Hence the length of the cylinder is 460mm. A rectangular flow domain is taken of height 460mm, width 460mm and length 1200mm. The tested cylinder is placed horizontally at the center of the rectangular flow domain. Coarse mesh for the whole geometry. Then named selection was done for the entire geometry. In this model have been meshed in the ansys14. By this 4010 hexahedra elements and 40 wedges were found as shown in Fig.2.2. Fig.2.3. shows the detailed view of meshed smooth circular cylinder captured from the rectangular flow domain.

2.2 MESHING GEOMETRY OF A CIRCULAR CYLINDER WITH V- GROOVES

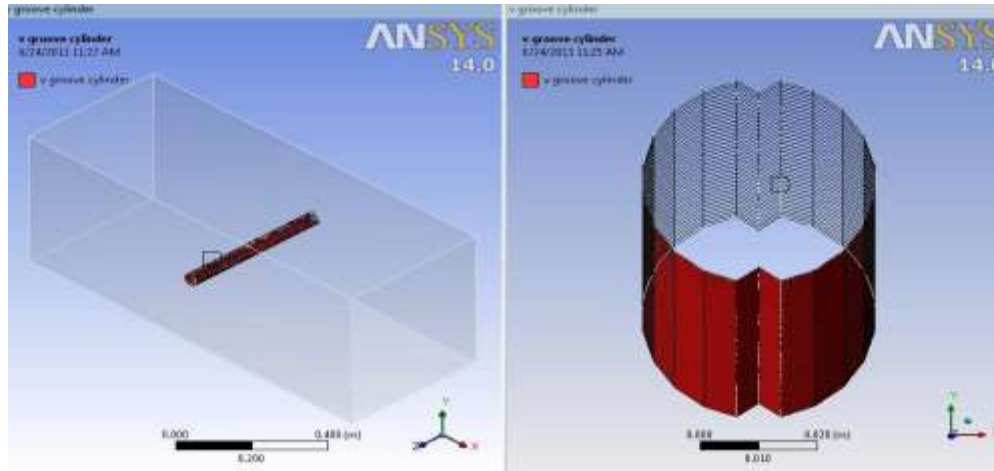


Fig.2.4: Meshed circular cylinder with V-grooves captured from the rectangular fluid flow domain

The modeling and geometrical parameters of circular cylinder with V-grooves remains same as smooth circular cylinder as shown in Fig.2.2. The only modification has been done on the surface of cylinder with V-grooves having 3mm depth and 110° angle as shown in Fig.2.4. The coarse mesh for the whole geometry having 15873 hexahedra elements and 222 wedge elements were obtained.

3. Results and discussion

3.1 NUMERICAL ANALYSIS OF SMOOTH CIRCULAR CYLINDER:

The experimental tests were performed for the following physical parameters for the circular cylinder^[1]:

- Reynolds number = 20000 (based on diameter and free-stream velocity).
- Free stream velocity (U_∞) = 7.5 m/s.
- Cylinder diameter = 40 mm
- Aspect ratios $L/D = 11.5$ in this study were investigated.

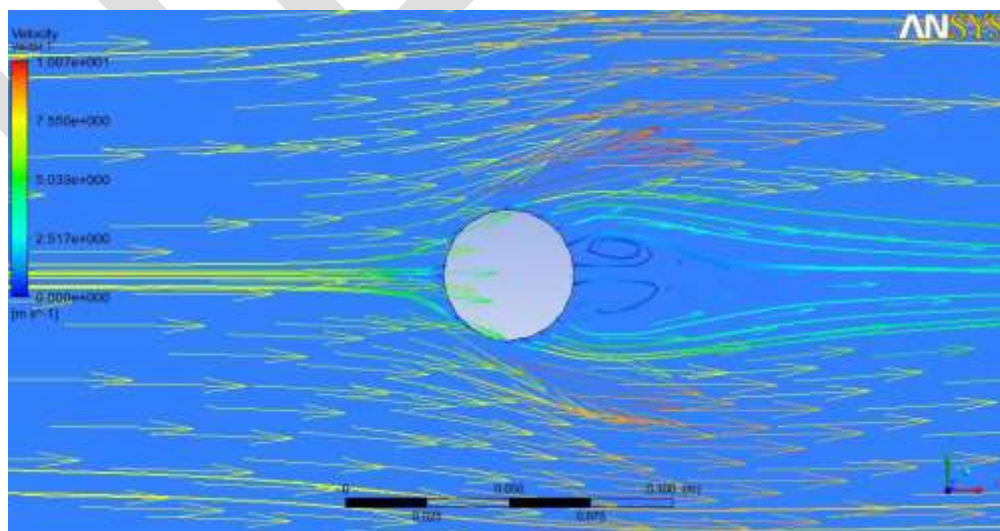


Fig. 3.1: Velocity vectors with stream lines for smooth circular cylinder

At Reynolds = 2×10^4 the flow pattern around the surface as shown in Fig. 3.1, The flow separates takes place in the downstream and a wake zone is formed by two symmetrical standing eddies. This gives rise to a zone of low pressure and the flow in this wake is highly turbulent and consisting of large eddies. High-rate energy dissipation takes place with the result that the pressure in the wake is reduced. A situation is thus created whereby the pressure acting on the front of the body is in excess of that acting on the rear of the body. The force arising from the pressure difference or more generally from the non-uniform pressure distribution on the body. The drag coefficient for the smooth cylinder is nearly constant and has an average value of 1.37. It agrees well with those of previous results measured in the ranges of $2 \times 10^4 < Re_D < 10^5$ nearly well-matched with the total drag coefficients at the same condition within the subcritical regime^[1].

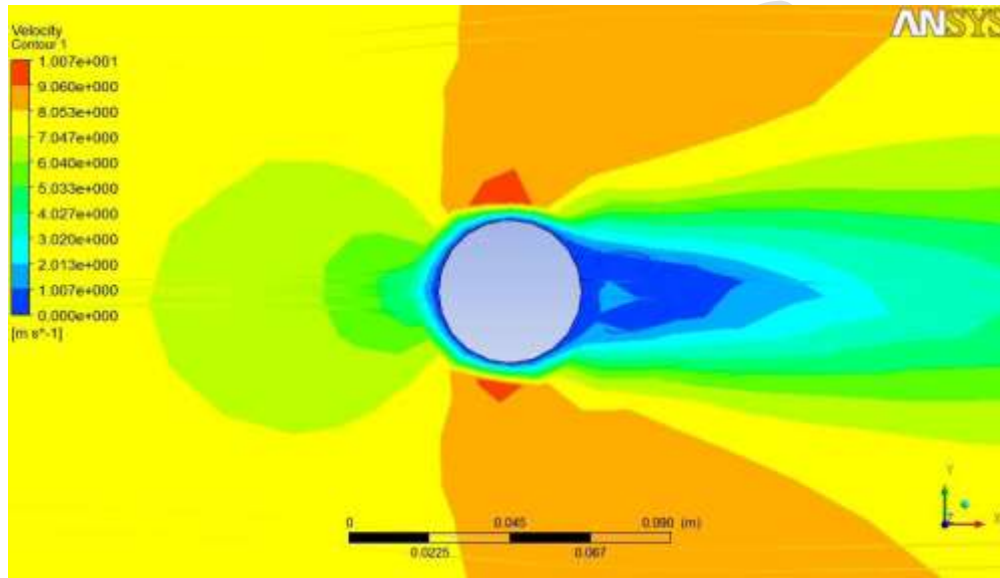


Fig.3.2: Velocity contours for a smooth circular cylinder

Fig.3.2 shows the velocity contours for a smooth circular cylinder. For a given cylinder, it was observed that velocity contours is maximum at top and bottom surface and minimum at back side of the cylinder. Because the velocity flow over the top and bottom is greater than free stream velocity.

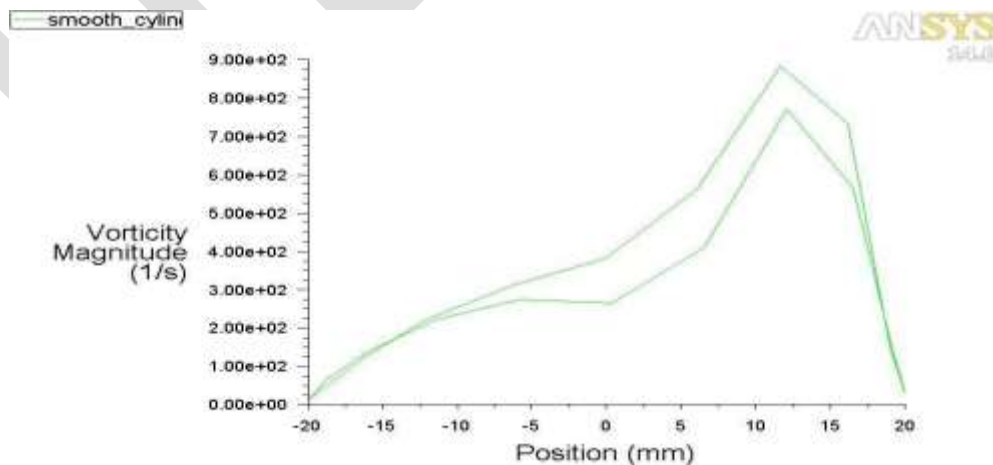


Fig.3.3: Vorticity magnitude v/s position of smooth circular cylinder

Fig.3.3 shows the vorticity magnitude v/s position of the smooth circular cylinder. From the Fig. It was observed that vorticity magnitude increases gradually upto to the sides of the cylinder and it is maximum at the point of wake formation. This gives rise to a wake zone of low pressure and the flow in this wake is highly turbulent and consisting of large eddies. High-rate energy dissipation takes place with the result that the pressure in the wake is reduced.

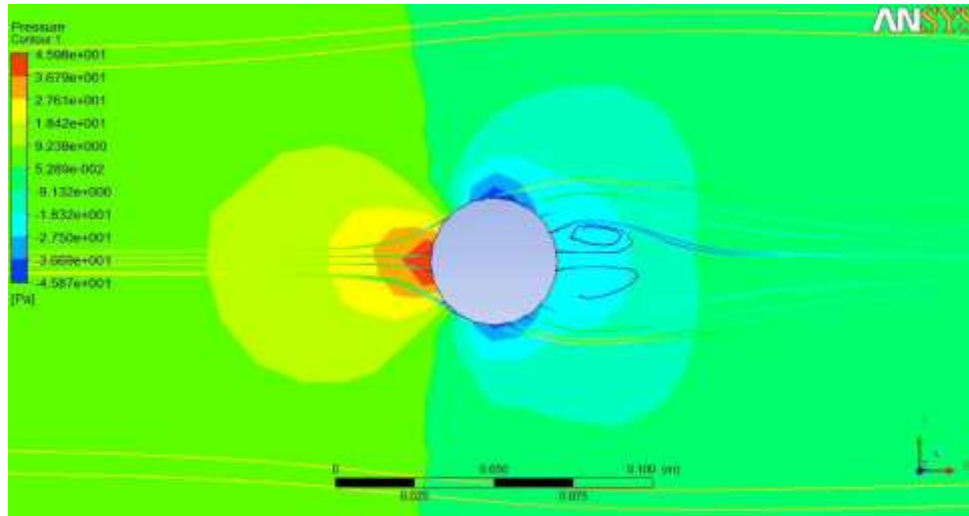


Fig. 3.4: Pressure contours for a smooth circular cylinder.

Fig.3.4 shows the maximum pressure at the front surface and minimum pressure at the back surface of the cylinder. High-rate energy dissipation takes place with the result that the pressure in the wake is reduced. A situation is thus created whereby the pressure acting on the front of the body is in excess of that acting on the rear of the body. The force arising from the pressure difference or more generally from the non-uniform pressure distribution on the body. As a result of pressure difference, drag will increase

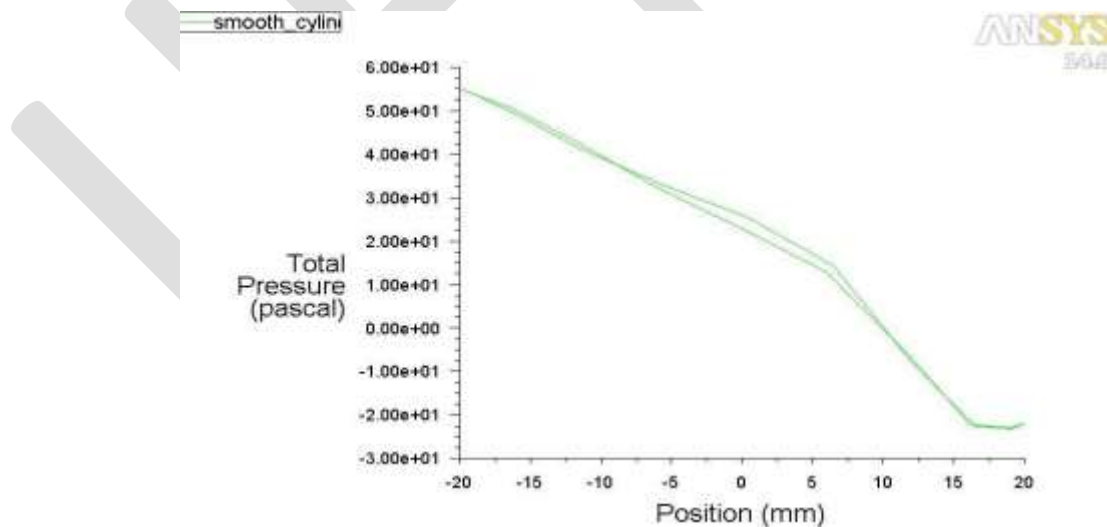


Fig 3.5: Total pressure contours for a smooth circular cylinder

Fig.3.5 shows total pressure curve for the smooth circular cylinder, as velocity increases, the boundary layer breaks away and eddies are formed behind. The drag becomes increasingly due to the pressure up at the front and pressure drop at the back of the cylinder. From the above Fig. it shows that how the total pressure decreases from front to back of the cylinder.

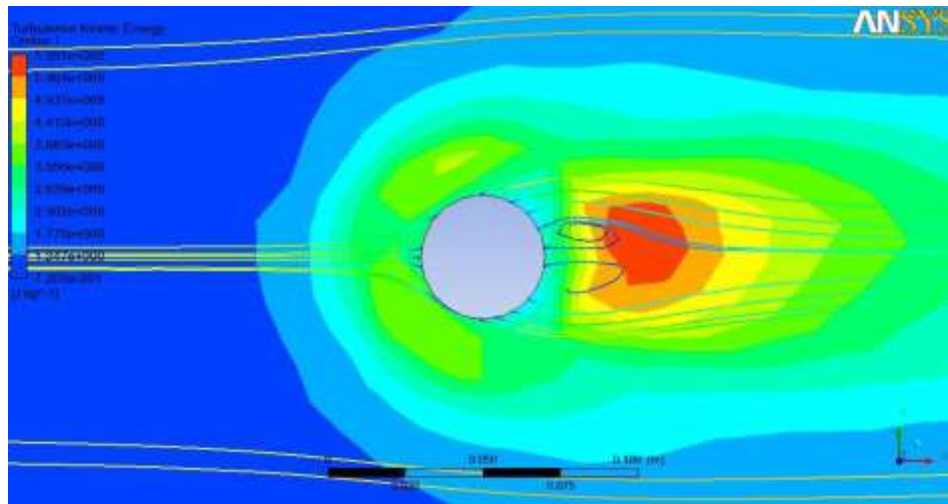


Fig.3.6: Turbulence kinetic energy for a smooth circular cylinder

Fig.3.6 shows that generation of wakes. Normally generation of wake takes place at the back side of the cylinder, turbulence kinetic energy is maximum at wake region and as a result of this smooth cylinder, most vorticity centers are uniformly distributed behind the cylinder. In addition to this, the smooth cylinder has larger number of vorticity at centers

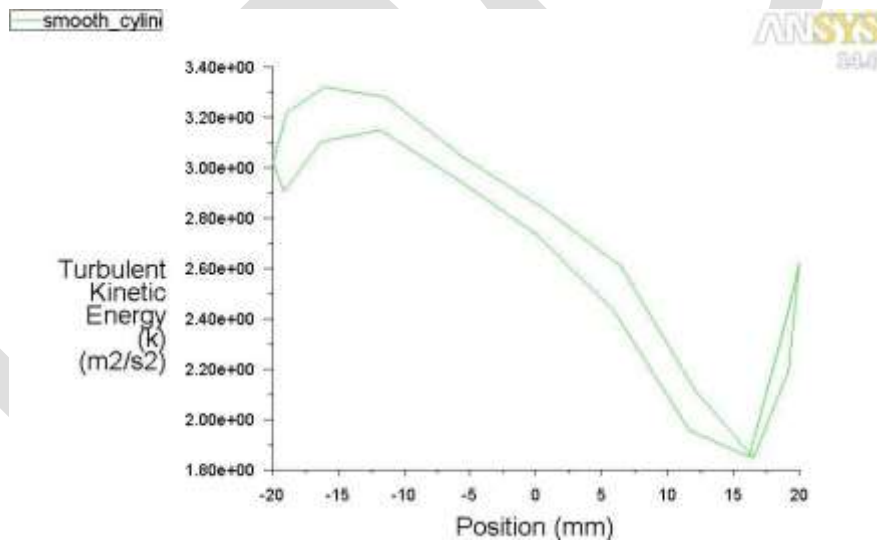


Fig.3.7: Turbulence kinetic energy v/s position of smooth circular cylinder

Fig.3.7 shows that turbulence kinetic energy uniformly decreases upto the point of wake region. After that, the turbulence kinetic energy increase due to the formation wake which results in the increase of drag coefficient.

3.2 NUMERICAL ANALYSIS OF CIRCULAR CYLINDER WITH V-GROOVES:

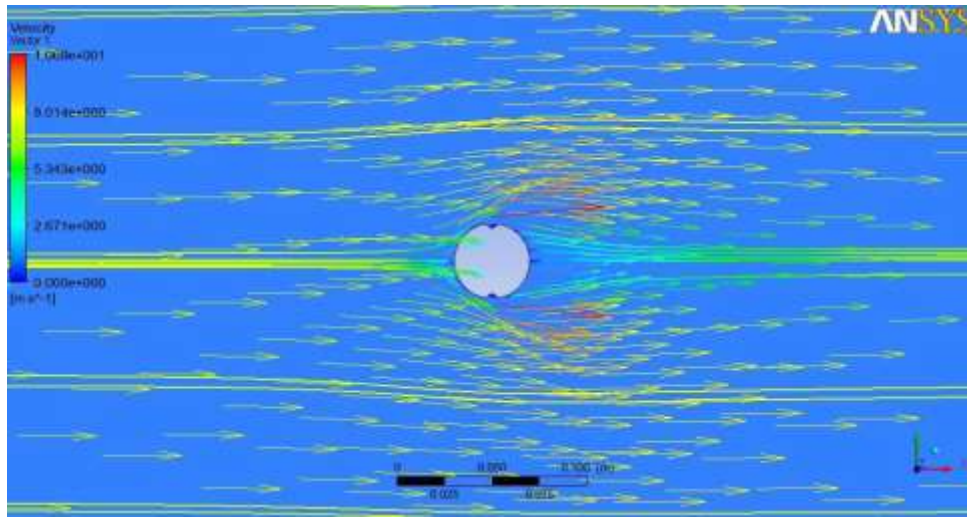


Fig.3.8: Distribution of velocity vectors and stream lines for a cylinder with V- groove

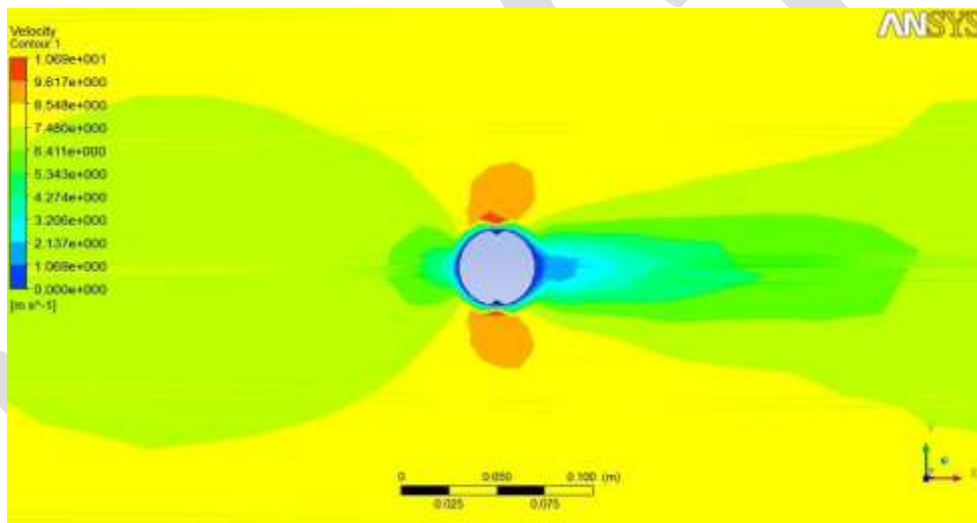


Fig.3.9: Velocity contours for a cylinder with V- groove

It appears that the flow pattern near the surface changes significantly due to the presence of grooves. Figs. 3.8 and 3.9, shows velocity vectors with stream lines and velocity contours. The vector plots indicate the presence of recirculation zones within the V- grooves, although Figs.3.8 and 3.9 contain recirculation zones. This indicates the presence of small-scale flow closer to the surface at high Reynolds numbers. At low Reynolds numbers the grooves create local recirculation zones filled with low momentum quiescent flow. These regions have decreased surface stresses and decreased pressure forces closer to the surface. This mechanism is absent in a smooth cylinder.

V- Grooves geometry for a smooth cylinder it is seen that, the viscous drag and lift forces decrease with increasing Reynolds numbers. At low Reynolds numbers ($Re = 20$ to 100) the presence of quiescent recirculation zones within the V - grooves lead to lower, which decreases the contribution of viscous forces. As the Reynolds number increases, smaller scales of motion are observed near the surface of V- groove cylinder which lead to higher. Therefore at a given Reynolds number the viscous forces decrease for a V- shaped groove cylinder in comparison to a smooth cylinder. The pressure forces do not change significantly at low Reynolds number. The pressure drag decreases by more than 28% at $Re (2 \times 10^4)$. It is speculated that, it is due to onset of three dimensional effects.

It is speculated that the effect of drag reduction in V- grooves cylinders will be less pronounced at significantly higher Reynolds numbers due to the presence of smaller turbulent length scales. At these high Reynolds numbers, a turbulent flow within the V- grooves will lead to a higher viscous forces near the surface, thereby reducing the effect of drag reduction mechanism. Since this behavior at significantly higher Reynolds numbers is explained based on the understanding at lower Reynolds numbers, the actual drag reduction mechanism might differ. It is therefore seen that the drag reduction is significantly higher at low Reynolds numbers and this grooves effect decreases with increasing Reynolds number.

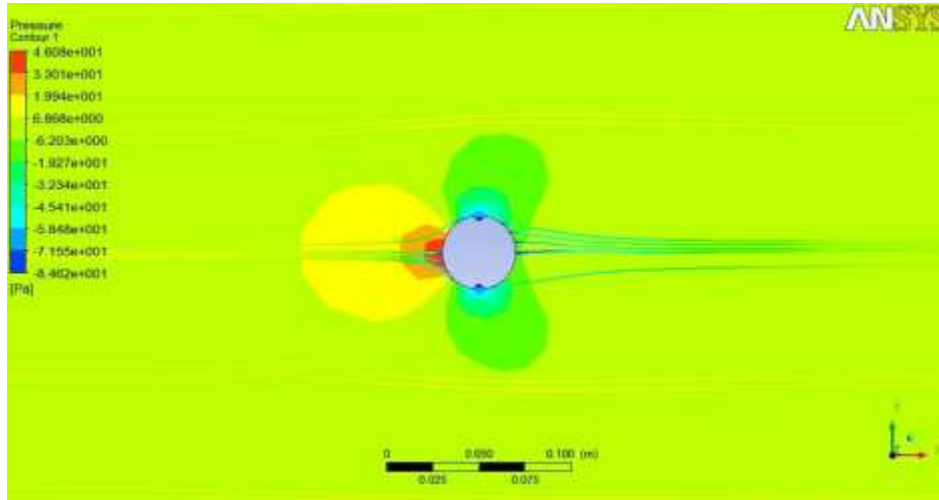


Fig.3.10: Pressure contours for cylinder with V- groove

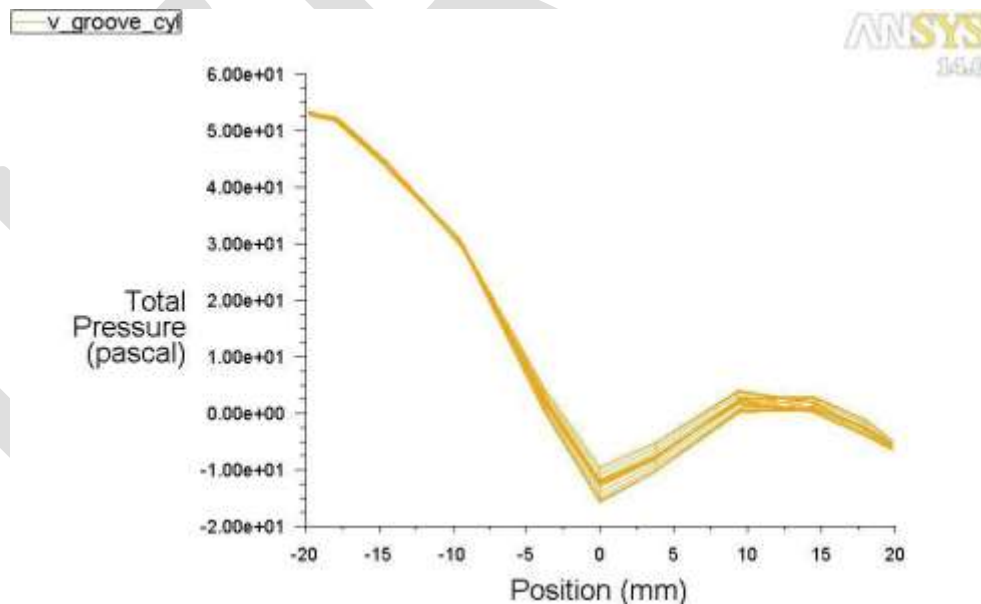


Fig.3.11: Total pressure distribution on cylinder with V – grooves

Pressure distributions at $Re = 20000$ for the cylinders, shown in Fig.3.10. There is greater pressure recovery for cylinders with cavities than for the smooth and rough cylinders. The cylinders with V- grooves have greater negative pressures on the sides of the cylinder. Pressure recovery appears to increase with increasing groove depth while the negative pressures on the sides of the cylinder appear not to be affected by groove depth. The pressure distribution depends somewhat on the orientation of the groove to the flow. When the groove trough faced the flow static pressures were very similar to those when the wall faced the flow. Conversely, when apex was

facing the flow, static pressures differed from those when the wall or groove trough faced the flow. The largest differences were for pressures on the front and sides of the cylinder. Fig.3.11 shows the total pressure curve for the V - groove cylinder. The pressure gradually decreases upto the position of V - grooves on cylinder surface. Due to this, there is a greater pressure recovery for sides of the cylinder.

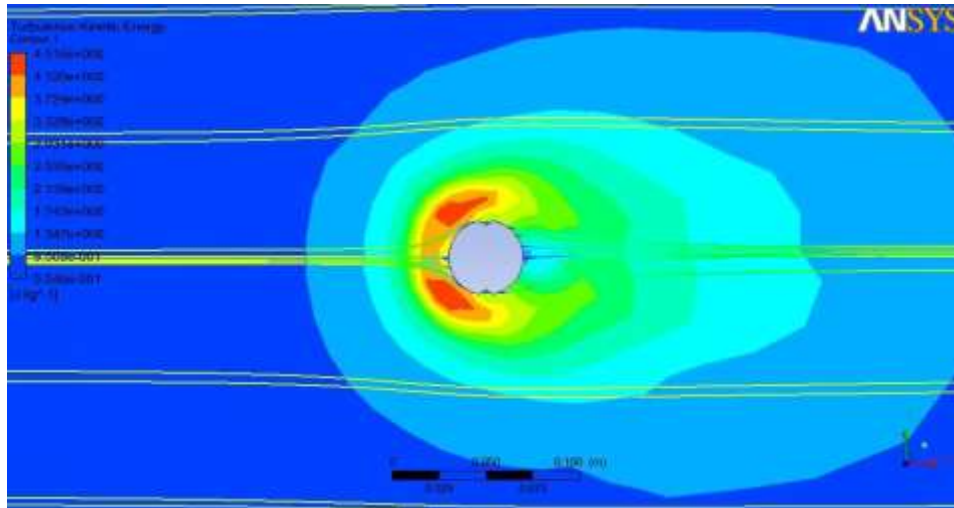


Fig.3.12: Turbulence kinetic energy for cylinder with V- grooves

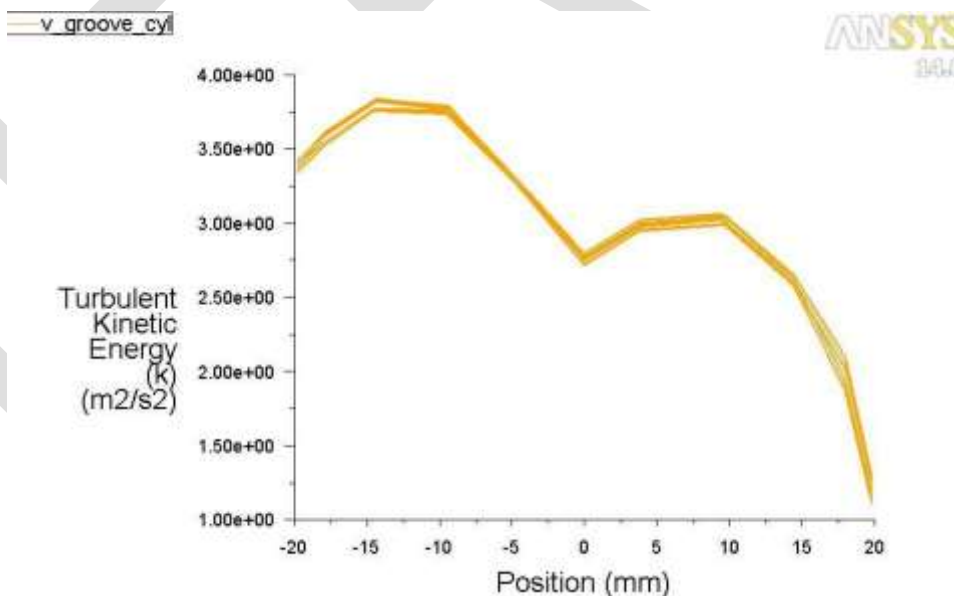


Fig.3.13: Turbulence kinetic energy v/s position of cylinder with V- grooves

Fig.3.12 shows the averaged turbulence kinetic energy distribution, the cylinder has large turbulence kinetic energy and regions of large and small kinetic energy exist together. However, the V - grooved cylinder seems to reduce the turbulence kinetic energy in the near wake. This may be attributed to the fact that formation of secondary vortices is suppressed in the region behind the V- grooved cylinder. The secondary vortices are broken into smaller eddies due to sharp peaks of the longitudinal V- shaped grooves. Fig.3.13

shows the turbulence kinetic energy v/s position of cylinder. The turbulence kinetic energy drops from back side of the V- grooves as there is less vortex formation.

3.3 DRAG COEFFICIENT AND V- GROOVE ANGLE STUDIES OF CYLINDER

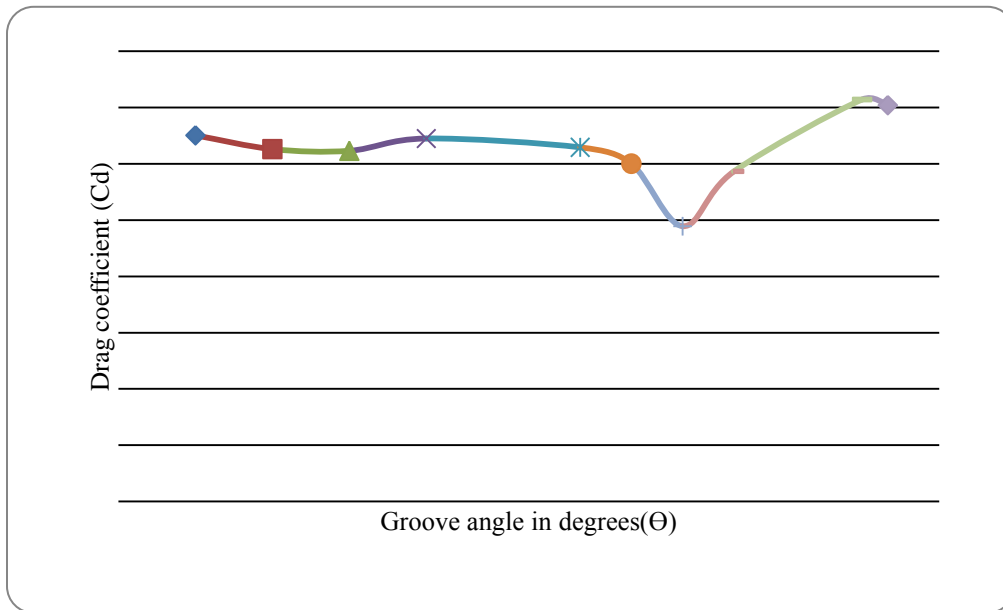


Fig.3.14: V- groove angle versus drag coefficient for cylinder with V- grooves

Fig.3.14 for the study of V – groove angle vary from 15 to 150° at constant groove depth and $Re = 2 \times 10^4$, The minimum drag coefficient is 0.9781 at an angle of 110° and 3mm depth and the maximum available drag coefficient is 1.4283 at an angle of 145°. The values of V – grooves on surface of circular cylinder from the table 3.1.

Table 3.1: Drag coefficient and v- groove angle studies on cylinder with V- groove

Groove angle in degree (Θ)	Groove Depth in mm (h)	Drag force in N (F _D)	Drag coefficient (C _d)
15	3	0.8247	1.3009
30	3	0.7937	1.2520
45	3	0.7899	1.2460
60	3	0.8176	1.2897
90	3	0.7977	1.2583
100	3	0.7609	1.2002
110	3	0.6201	0.9781
120	3	0.7436	1.1729
145	3	0.9055	1.4283
150	3	0.8926	1.4080

CALCULATION:

At 110 ° V - groove angle and 3mm depth

From fluent data the properties of fluid, fluid as air given below

$$\rho = 1.225 \text{ kg/m}^3, \mu = 1.7894 \times 10^{-5} \text{ kg/m-s}$$

Physical parameters:

$$D = 40\text{mm}, L = 460\text{mm}, S = D \times L$$

Formula for drag coefficient:

$$C_d = \frac{2F_D}{\rho \times U^2 \times S}$$

$$= \frac{2 \times 0.6201}{1.225 \times 7.5^2 \times 0.04 \times 0.46}$$

$$= \frac{1.2402}{1.2679}$$

$$= 0.9781$$

Table 3.2: Drag coefficient and V- grooves depth on cylinder with V-grooves

Angle in degree (Θ)	Groove depth in mm (h)	Drag force in N (F _D)	Drag coefficient (C _d)
110	2	0.7276	1.1477
110	3	0.62008	0.9781
110	4	0.6862	1.0824
110	5	0.7264	1.1458

Table 3.2 the study of V – groove depth vary from 2 to 5mm at constant groove angle, the numerical results are obtained as shown in the table 3.2. In this study had conclude that the minimum drag coefficient is obtained at an angle 110 ° and 3mm depth, further increases the groove depth, the drag force also increases for this studies.

ACKNOWLEDGMENT

I express my sincere thanks and heartfelt gratitude to my guide, Mr. Kishan Naik for their, inspiration, guidance and support during this project work. I thank my parents & friends for their moral support.

CONCLUSION

The flow structure of wake behind a circular cylinder with longitudinal V-grooves has been investigated numerically using CFD tool techniques.

- The V-grooved cylinder reduces the drag coefficient by about 28.47% at Re_D = 2 × 10⁴, compared with the smooth cylinder at same Reynolds number.
- The drag reduction of the V- grooved cylinder increases with increasing Reynolds number.
- The vortex formation region behind V- grooved cylinder is smaller than for the smooth cylinder.
- The longitudinal grooves seem to reduce the size of spanwise vortices and shift their location toward the cylinder. The sharp peaks of longitudinal V- shaped grooves also suppress the formation of large-scale secondary streamwise vortices.
- The secondary vortices are broken into smaller eddies, reducing the turbulence kinetic energy in the near-wake region.

REFERENCES:

- [1] Ladjedel A.O, Yahiaoui B.T, Adjlout C.L and Imine D.O, “ Experimental and Numerical Studies of Drag Reduction on a Circular Cylinder”, World Academy of Science, Engineering and Technology 53 2011.
- [2] Zhang H.L, and N.W.M. KO, “Numerical Analysis Of Incompressible Flow Over Smooth And Grooved Circular Cylinders”, Department of Mechanical Engineering, The University of Hong Kong, Pokfulam Road, Hong Kong, 1995.
- [3] Lim H.C, Lee S.J, “PIV Measurements Of Near Wake Behind A U-Grooved Cylinder”, Journal Of Fluids And Structures 18 (2003) 119–130.
- [4] Carmo B.S, Meneghini J.R, “Numerical Investigation Of The Flow Around Two Circular Cylinders In Tandem”, Journal of Fluids and Structures 22 (2006) 979–988.
- [5] Steven J. Quintavalla , Alexander J. Angilella, Alexander J. Smits , “ Drag Reduction On Grooved Cylinders In The Critical Reynolds Number Regime”, Experimental Thermal and Fluid Science 48 (2013) 15–18.
- [6] Ming Zhao, Liang Cheng, Bin Teng, Dongfang Liang, “Numerical Simulation Of Viscous Flow Past Two Circular Cylinders Of Different Diameters”, Applied Ocean Research 27 (2005) 39–55.
- [7] Pietro Catalano, Meng Wang, Gianluca Iaccarino, Parviz Moin, “The Viability And Accuracy Of Large-Eddy Simulation (LES) With Wall Modeling For High Reynolds Number Complex Turbulent Flows Is Investigated By Considering The Flow Around A Circular Cylinder In The Supercritical Regime” International Journal of Heat and Fluid Flow 24 (2003) 463–469.
- [8] Braza M, Perrin R, Hoarau Y, “Turbulence Properties In The Cylinder Wake At High Reynolds Numbers”, Journal of Fluids and Structures 22 (2006) 757–771.
- [9] Pradeep Babu and Krishnan, Mahesh, “Aerodynamic Loads On Cactus Shaped Cylinders At Low Reynolds Numbers”, Physics Of Fluids 20, 035112 (2008).
- [10] Tsutsui T, Igarashi T, “Drag Reduction Of A Circular Cylinder In An Air-Stream”, Journal of Wind Engineering and Industrial Aerodynamics 90 (2002) 527–541.
- [11] Sharon Talley and Godfrey Mungal, “Flow Around Cactus-Shaped Cylinders” Center for Turbulence Research Annual Research Briefs 2002.
- [12] Fujisawa N, Asano Y, Arakawa C, Hashimoto T, “Computational And Experimental Study On Flow Around A Rotationally Oscillating Circular Cylinder In A Uniform Flow”, Journal of Wind Engineering and Industrial Aerodynamics 93 (2005) 137–153
- [13] Igbalajobi A, McClean J.F, Sumner D, Bergstrom D.J, “The Effect Of A Wake Mounted Splitter Plate On The Flow Around A Surface-Mounted Finite-Height Circular Cylinder”, Journal of Fluids and Structures 37 (2013) 185–200.
- [14] Nakamura H, Igarashi T, “Omnidirectional Reductions In Drag And Fluctuating Forces For A Circular Cylinder By Attaching Rings” Journal of Wind Engineering and Industrial Aerodynamics 96 (2008) 887–899.
- [15] Viswanath P.R, “Aircraft Viscous Drag Reduction Using Riblets” Progress in Aerospace Sciences 38 (2002) 571–600.
- [16] Shan Huang, “Omcircular Cylinder And Drag Reduction Of A Fixed Circular Cylinder By The Use Of Helical Grooves”, Journal of Fluids and Structures 27 (2011) 1124–1133.
- [17] Mutschke G, Shatrov V, Gerbeth G, “Cylinder Wake Control By Magnetic Fields In Liquid Metal Flows” Experimental Thermal and Fluid Science 16 (1998) 92-99.
- [18] Aswatha Narayana P. A, Seetharamu K. N, “Engineering Fluid Mechanics”, text Book, Alpha science international, 2004